Steel and Composite Structures, *Vol. 32, No. 5 (2019) 559-569*
DOI: https://doi.org/10.12989/scs.2019.32.5.559

An experimental investigation on effect of elevated temperatures on bond strength between externally bonded CFRP and concrete

Behzad Attari [a] and Mohammadreza Tavakkolizadeh[*]

Department of Civil Engineering, Ferdowsi University of Mashhad, Mashhad, Iran

(*Received April 14, 2018, Revised January 29, 2019, Accepted August 21, 2019*)

Abstract. The bond strength between composite laminates and concrete is a key factor that controls the behavior of concrete members strengthened with fiber reinforced polymer (FRP) sheets, which can be affected by several parameters such as thermal stresses and surface preparation. This article presents the result of an experimental study on the bond strength between FRP sheets and concrete at ambient temperature after specimens had been exposed to elevated temperatures of up to 200℃. For this purpose, 30 specimens of plain concrete with dimensions of 150×150×350 mm were prepared. Three different conventional surface preparation methods (sandblasting, wire brushing and hole drilling) were considered and compared with a new efficient method (fiber implantation). Deformation field during each experiment was monitored using particle image velocimetry. The results showed that, the specimens which were prepared by conventional surface preparation methods, preserved their bond integrity when exposed to temperature below glass transition temperature of epoxy resin (about 60℃). Beyond this temperature, the bond strength and stiffness decreased significantly (about 50%) in comparison with control specimens. However, the specimens prepared by the proposed method displayed higher bond strengths of up to 32% and 90% at 25℃ and 200℃, respectively.

Keywords: FRP; temperature; bond strength; fiber implantation; PIV

1. Introduction

Fiber Reinforced Polymers (FRP) have received significant attention for rehabilitation of civil infrastructure due to their outstanding physical and mechanical properties. The most common method of strengthening structural member using FRP composites is the externally bonded reinforcement (EBR) method. Despite the several advantages of the EBR method, the main weakness of this technique is the premature FRP debonding from concrete substrate and consequently, failure to utilize the maximum FRP tensile capacity (Cheng *et al*. 2002).

Many studies have focused on improving the performance of EBR technique, postponing the debonding failure, and making better use of high tensile capacity of FRPs.

Spadea *et al*. (1998) sugested that the providing adequate anchorages at the ends of the plates and at critical sections along the span are necessary to obtain maximum benefit from the CFRP plate. Grace *et al*. (1999) indicated that in addition to instation of FRP sheets in longitudinal direction, FRP strips in transverse direction forming a U-shape around the beam cross section, significantly reduce beam deflections and increase its load carrying capacity. Mostofinejad and Hajrasouliha (2010) suggested the grooving method as an alternative to the EBR and showed the influence of this method to postpone debonding from the concrete substrate was significant. Over the past decade, near surface mounting (NSM) technique has been also introduced as a valid alternative to externally bonded FRP sheets (Carolin *et al*. 2001, De Lorenzis 2004, Barros and Fortes 2005). Although further studies have reported better performance of NSM technique (Nordin and Taljsten 2006, Hajihashemi *et al*. 2011), debonding is yet the major problem in both NSM and EBR methods and has remained as an important drawback in using FRP materials for flextural rehabilitation of reinforced concrete structures.

Many different experimental set-ups have been used to determin the FRP-concrete bond strength, but no consensus on a standard test procedure has been reached. Chen and Teng (2001) classified the existing test set-ups into three types (see Fig. 1) as: (a) double-shear tests (like double-lap shear test); (b) single-shear tests (this set-up was used in this study); (c) bending tests.

According to Malek *et al*. (1998), Kim *et al*. (2012), and Hadji *et al*. (2016), premature debonding failure initiates due to high tensile and shear stresses caused by mechanical and environmental loading between the surface of FRP and concrete substrate. Environmental loads can be caused by cycles of wetting and drying, freezing and thawing or temperature variations (Burke *et al*. 2013). Due to the significant differences in coefficients of thermal expansion of FRP sheets and concrete, when the strengthened system is exposed to elevated temperatures, thermal stresses occurs at the interface of concrete surface and the FRP sheet (Xin *et al*. 2015). The mechanical properties of the adhesive and CFRP sheets and the bond between sheets and concrete

*Corresponding author, Ph.D., Assistant Professor,
E-mail: drt@um.ac.ir
[a] Ph.D. Student

ISSN: 1229-9367 (Print), 1598-6233 (Online)

substrate would also change at different temperature (Firmo *et al*. 2015a). This applies to most polymers, as their strength and stiffness drop significantly when the glass-transition temperature (Tg) is reached (45–80℃ for most cold cured polymers). Changing material properties and thermal stresses due to difference in the coefficient of thermal expansions may affect the load level at which debonding occurs (Klamer *et al*. 2007).

Despite the importance of the issue, limited research has been conducted on this matter so far. Some studies focused on the bond strength during the exposure to elevated temperatures, and a few studies were concentrated on the bond strength when system had been exposed to elevated temperatures. Blontrock (2003) evaluated the bond strength of CFRP strips and concrete using the double-lap shear test at temperatures of 20℃, 40℃, 55℃, and 70℃. The adhesive used to externally bond the CFRP strips had a Tg of 62℃ (test method was not specified). The changes in bond strength at 40℃, 55℃, and 70℃ compared to the strength at 20℃ was 141%, 124%, and 82%, respectively. The reason given for these results, was the thermal stress created between the surfaces of CFRP and concrete caused by the difference in their coefficient of thermal expansion. Klamer *et al*. (2005) presented a similar conclusion. In this study, they evaluated the bond strength of CFRP strips to concrete at a temperature range of -10℃ to 75℃ by conducting a double-lap shear test. They used normal concrete and epoxy resin with a Tg of 62℃ (values were provided by the manufacturer without specifying test method) to prepare the specimens. Specimens were exposed to heat for 12 hours before loading. They also reported a 10% increase in bond strength up to a temperature of 50℃ and a 36% reduction in bond strength at a temperature of 75℃. Klamer (2009) presented results of a follow-up study, with specimens made of both normal and high strength concrete and tested at temperature of -20℃ to 90℃. They reported a similar result compare to their original study. Wu *et al*. (2005) performed similar double-lap shear test, at a temperature range of 26℃ to 50℃, in order to measure the bond strength of the CFRP and concrete. The Tg of the epoxy resin used by them was about 38℃ (test method not specified). Unlike other studies, with increasing temperature, they reported a decrease in bond strength (60% decrease at 50℃). Leone *et al*. (2009) performed double-lap shear tests on concrete blocks with either CFRP strips or sheets, both externally bonded with epoxy adhesive (Tg of 55℃, determined from differential scanning calorimetry). Tests were performed at tempera-tures ranging from 20℃ to 80℃. In addition to high high scatters, a non-monotonic variation of bond strength with temperature was reported for the CFRP strips. This differedfrom results by other researchers (Blontrock 2003, Klamer *et al*. 2005 and Klamer 2009). Bond strength retentions decreased and increased below and above their Tg, respectively. Firmo *et al*. (2015b) performed double-lap shear tests on concrete blocks with externally bonded CFRP strips (Tg of 47℃, determined by DMA) from 20℃ up to 120℃. The effect of using a mechanical anchorage on the extremities of the CFRP strips was also investigated. They concluded that increasing temperature caused significant reduction of bond strength. Namrou (2013) conducted an experimental study on the effect of temperature on the adhesion strength of three types of epoxy resin to concrete. The Tg of the epoxy resins were 65℃, 75℃ and 165℃ (determined by DMA). In this study, first the specimens were exposed to a range of temperatures (25 to 200℃ for three hours and then, tests were conducted at ambient temperature). The bond strength did not change up to temperatures lower than Tg, but after passing this threshold, capacities rapidly decreased 50% and then remained almost constant. Al-Salloum *et al*. (2011) conducted a laboratory research on the bond strength of CFRP and GFRP sheets to concrete after exposure to high temperatures. The Tg of the used epoxy resin was about 88℃ (ASTM D3418–08 was used to evaluate the Tg). They exposed the specimens to two temperatures of 100℃ and 200℃ for three hours, and then the bond strength between sheets and concrete substrates was measured at ambient temperature using the pull-off test. Based on their results, bond strength was significantly decreased when exposed to a temperature of 200℃. Also, the reduction of bond strength in specimens prepared with CFRP sheets was more than that of specimens prepared with GFRP sheets.

By reviewing previous studies, it can be concluded that with increasing temperature beyond Tg, the bond strength would be reduced, but the amount of this reduction varied in different cases. Also, there were inconsistent results for the behavior of bond below Tg. In some studies, at temperatures below Tg, bond strengths were increased (Blontrock 2003, Klamer *et al*. 2005, 2009), while in others bond strengths were decreased (Wu *et al*. 2005, Leone *et al*. 2009). The methods for testing the bond strength were different in the literature. Additionally, no methods have been recommended to prevent the unpleasant phenomenon of premature debonding of the FRP sheets from the concrete substrate after exposure to elevated temperature. In this study, the effect of surface preparation and elevated

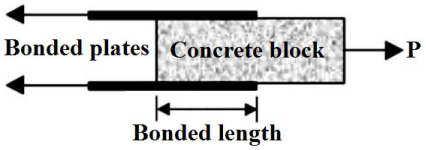

(a) Double-shear tests

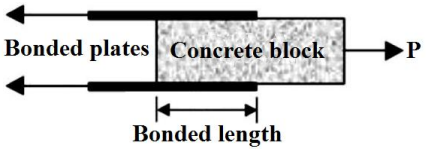

(b) Single-shear tests

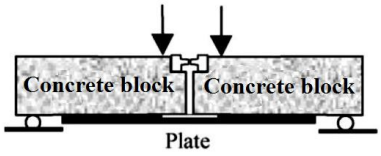

(c) Bending tests

Fig. 1 Classification of bond tests (Chen and Teng 2001)

temperature on CFRP-concrete bond strength were investigated by performing a single-shear test to measure the bond strength. A new strengthening method was also proposed to postpone or completely eliminate the premature exposure to elevated temperatures.

2. Experimental procedure

2.1 Material characteristics

In order to perform single-shear tests, 30 concrete specimens with dimension of 150×150×350 mm were prepared. Concrete mix design to give a compressive strength of about 30 MPa was consisted of 350 kg/m3 of Portland cement type I, 811 kg/m^3 sand, 887 kg/m^3 gravel and 182 kg/m^3 water without any additive. Moreover, to determine the compressive strength of concrete, three concrete cylinders with dimensions of 150×300 mm were prepared from each mix. Specimens were demolded after 24 hours and were kept in lime saturated water for 27 more days. Subsequently, all specimens were removed from the water and kept inside laboratory until the date of testing. The CFRP sheets used in this study was fabricated by wet layup process using Kor-CFW200 unidirectional carbon fabric. According to the recommendation by manufacturer, two-component epoxy EPIKOTE 828 with a Tg of about 60℃ (values provided by the manufacturer) was used as CFRP matrix and for bonding CFRP sheet to the concrete substrate. The mechanical properties of carbon fibers, epoxy resin and CFRP sheets used in this study are tabulated in Table 1 based on the manufacturer data sheet. It should be noted that the tensile strength of the CFRP sheet made by the wet layup process would be much lower than the tensile strength and modulus of carbon fibers presented in Table 1. Ultimate Tensile capacity (load per unit width) of the composite used in this study as reported by the manufacturer was 432 N/mm.

2.2 Specimens dimensions and preparation

In this research, the effect of concrete surface preparation and the exposure to elevated temperature on the bond strength of CFRP sheets and concrete substrate was investigated. Other factors affecting the bond strength of the CFRP sheets and the concrete, remained constant. Names of specimens was designated in the form of A-B-C-D, in which "A" represented the strengthening technique (CO for conventional, HL for hole drilling and FI for fiber implantation), "B" represented the type of surface preparation of the concrete substrate (S for sandblasted, B for wire brushed and N for none), "C" represented the temperature of the test in degree Celsius and "D" represented the ordinal number of each test (1 or 2). Two examples were presented in Table 2.

Conventional (CO) Specimens: In order to prepare specimens using this technique, first the weak layer of the cement paste was removed from concrete surface by either sandblasting or wire brushing and after cleaning the surface by compressed air, a layer of carbon fabric with 50 mm width was adhered to the prepared concrete surface (bonded length of 150 mm) using epoxy resin with wet layup procedure as shown in Fig. 2. The bond length was selected twice the effective bond length obtained from the model suggested by Chen and Teng (2001), (Eq. (4)).

Hole Drilled (HL) Specimens: In order to prepare specimens using this technique, first the weak layer of the cement paste was removed from concrete surface by wire brush and then three holes with a diameter of 10 mm and depth of 40 mm were drilled into the concrete, 50 mm apart(center to center). After cleaning inside the holes with the compressed air, they were filled with epoxy resin and

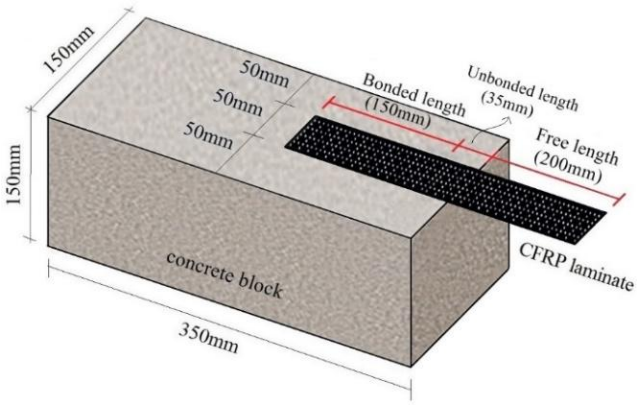

Fig. 2 Test specimen

Table 1 Properties of FRP component

	Product name	Thickness (mm)	Tensile strength (MPa)	Elastic modulus (GPa)	Elongation at beak (%)
Fibers	Kor-CFW200	0.11	4900	230	1.8
Adhesive	EPIKOTE 828	-	35	4.0	2.0
Composite	CFRP Sheet	0.20	1850	125	1.4

Table 2 Specimens naming

Specimen name	Strengthening technique	Surface preparation	Temperature	Ordinal number
CO-B-25-1	Conventional	Wire brushed	25℃	1
FI-N-25-2	Fiber implantation	none	25℃	2

(a) Hole preparation

(b) Fibers implantation

(c) Implanted strands direction

Fig. 3 Strengthening using fiber implantation method

one layer of carbon fabric with 50 mm width was adhered to concrete surface using epoxy resin with wet layup procedure. It worth noting that geometry of the holes was chosen based on past experience and a few unpublished preliminary studies.

Fiber Implanted (FI) Specimens: Twelve specimens were prepared using a proposed method to better bond the CFRP sheets to concrete and prevent the undesirable phenomenon of premature debonding at ambient or elevated temperature. As shown in Fig. 3, to prepare the specimens, first the holes with a diameter of 10 mm and depth of 40 mm were drilled into the concrete, 50 mm apart (center to center) and after cleaning inside the holes with the compressed air, carbon fiber strands with the length 80 mm were implanted inside the holes using epoxy resin so that half of their length buried inside the hole and other half stayed outside. Then, the free part of the strand was bent and adhered to concrete surface in direction of applied tensile load. Finally, one layer of carbon fabric with 50 mm width was adhered to concrete surface using epoxy resin with wet layup procedure on top of the implanted strands in order to developing better bond. In order to further demonstrate the effectiveness of the proposed technique, two types of specimens were made (concrete surface without any preparation or with wire brushing). It should be noted that geometry of the holes and fiber strands were chosen based on past experience and a few unpublished preliminary studies. Holes were deep enough to penetrate the concrete beyond the typical cover thickness. Diameter of holes were wide enough to make strand insertions simple and practical. Strands were long enough to cover the area between holes without overlapping and interfering with each other.

Fig. 4 Spreading natural colored sand before setting of the epoxy

In order to acquire deformation measurements using advanced technique of image processing, it was necessary to take several images from the desired surface using the still camera during loading. The surface should have rough texture if points to be recognized by analyzing software readily (Hosseini and Mostofinejad 2013). Since the CFRP sheets did not have desirable texture, colored sand with grain size of between 0.15 and 0.30 mm were used to generate detectable roughness in this study. The colored sand was spread on top of the CFRP sheet before the epoxy started to cure as shown in Fig. 4.

After curing of epoxy resin at ambient temperature for 3 weeks (suggested curing requirement by manufacturer was 7 days), the specimens were placed in an oven for three hours (at 25, 50, 100, 150 and 200℃ with temperature history presented in Fig. 5) and then, they were left outside at ambient temperature for 24 hours.

2.3 Test setup, instrumentation and procedure

According to the research by Al-Salloum *et al*. (2011), specimens were exposed to different temperature and kept for three hours in an oven. The air inside the oven was circulated by a fan and temperature was controlled by a digital thermometer with a precision of 0.01℃. The apparatus for conducting single-shear tests was designed and fabricated as shown in Fig. 6. A positioning frame was used to prevent the far end of the concrete prism from uplifting. After placing the specimens inside the test frame, a hydraulic jack with a capacity of 300 kN applied the tensile force to the CFRP sheets using a friction type grip

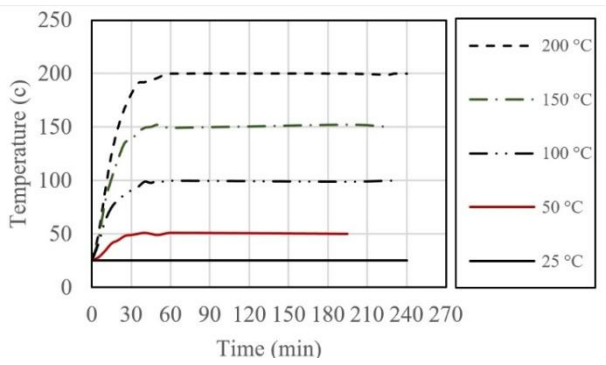

Fig. 5 Time–temperature curves used in this study

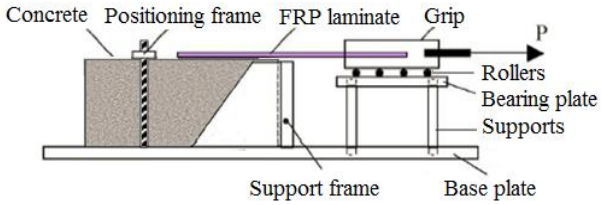

(a) Longitudinal section of test setup (Schematic)

(b) Image of the test set up

Fig. 6 Single-shear pull test apparatus

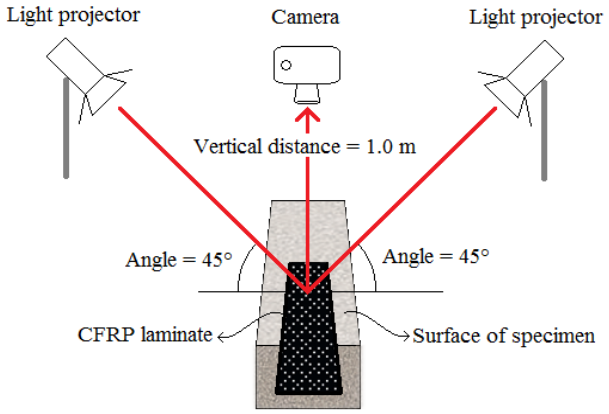

Fig. 7 Positions of camera and light projectors

until its failure. According to ASTM D3039 (2000) recommendation, all tests were performed under displacement control with a rate of 2.0 mm/min.

During loading, images from the upper surface of a specimen was taken using a Canon-EOS-1300D digital camera with a resolution of 18.0 megapixels (3456×5184 pixels), equipped with a Canon 18-55 lens (exact focal lens used in the tests was 35 mm) at a distance of one meter away from the surface. Two light projectors on either side of the specimen were used to eliminate any probable light infractions as shown in Fig. 7. In order to minimize the stress concentration and the loaded end of the CFRP sheets, a 35 mm unbonded area was considered following the suggestion made by other researchers (Ali-Ahmad *et al*. 2006 and Mazzotti *et al*. 2008).

3. Image analysis using particle image velocimetry (PIV)

In this study, the particle image velocimetry (PIV) measurement method was used to determine the deformation field of CFRP sheets under loading. At first, PIV was a velocity-measuring technique established in fluid mechanics for experimental and field measurements (Adrian 1991). White *et al*. (2003) expanded the PIV method with a series of modifications for using in geotechnical experiments. Based on the validation performed by White *et al*. (2003), Slominski *et al*. (2007) and Hajialilue-Bonab *et al*. (2011), the modified PIV technique compared with the earlier techniques used to measure displacement, increases accuracy, precision and the measurement array size. PIV analysis procedure can be summarized as:

- Subdivide the first image and select a test patch.
- Determine the correlation and normalize the test patch using FFT and mask function.
- Find sub-pixel location of correlation peak using bicubic interpolation.
- Repeat the process for all images and to develop displacement vector.
- Use displacement field and set up strain tensor.

In this study, deformations in the CFRP sheets were recorded using digital imaging during the test. The images were then analyzed using the geoPIV_RG software developed at Cambridge University (White and Take 2002). Patches of 128×128 pixels spaced at 32 pixels apart (center-to-center) were used for PIV analysis. For all PIV analysis, a 5×5 pixel search area was considered for each pair of successive images to provide a sufficient area to track patches. According to White *et al*. (2003), the precision of the PIV is a function of the patch sizes. Using 128×128 pixels patches, conservatively, delivered an accuracy of about 0.005 pixel by considering an 18-megapixel (3456×5184 pixels) camera. Therefore, the displacement measurement accuracy of this study was more than 0.5 μm.

4. Results and discussion

Experimental ultimate failure load, P_{exp}, compressive strength of concrete, f'_c and failure mode of all specimens were presented in Table 3. The calculated failure loads, P_{cal}, were also calculated by the model presented by Chen and Teng (2001) and compared with the experimental ultimate load measured during each test. The calculated ultimate load of the FRP sheet is

$$P_{cal} = \alpha \beta_w \beta_l b_f L_e \sqrt{f'_c} \tag{1}$$

$$\beta_w = \sqrt{\frac{2 - b_f/b_c}{1 + b_f/b_c}} \tag{2}$$

$$\beta_l = \begin{cases} 1.0 & if\ L_f \geq L_e \\ \sin\frac{\pi}{2}\frac{L_f}{L_e} & if\ L_f < L_e \end{cases} \tag{3}$$

$$L_e = \sqrt{\frac{E_f t_f}{\sqrt{f'_c}}} \tag{4}$$

Table 3 Details of specimens and test results

Test specimen	f'_c (MPa)	P_{exp} (kN)	P_{exp}/P_{cal}	Test failure mode[a]	Average P_{exp} (kN)
CO-B-25-1	31.2	9.41	1.01	DB-C	9.56
CO -B-25-2	31.2	9.71	1.04	DB-C	
CO -B-50	31.2	9.61	1.03	DB-C	-
CO -B-100	31.2	6.18	0.66	DB-I	-
CO -B-150	31.2	5.61	0.60	DB-I	-
CO -B-200	31.2	4.79	0.51	DB-I	-
CO -S-25-1	31.2	9.30	1.00	DB-C	9.45
CO -S-25-2	31.2	9.61	1.03	DB-C	
CO -S-50	31.2	9.51	1.02	DB-C	-
CO -S-100	31.2	5.65	0.60	DB-C	-
CO -S-150	31.2	5.60	0.60	DB-I	-
CO -S-200	31.2	*	-	DB-I	-
HL-B-25-1	29.7	9.66	1.06	DB-C	9.58
HL-B-25-2	29.7	9.50	1.05	DB-C	
HL-B-50	29.7	9.1	1.00	DB-C	-
HL-B-100	29.7	6.21	0.68	DB-I	-
HL-B-150	29.7	5.97	0.66	DB-I	-
HL-B-200	29.7	4.95	0.54	DB-I	-
FI-N-25-1	30.6	13.02	-	RU	12.71
FI-N-25-2	30.6	12.40	-	RU	
FI-N-50	30.6	12.82	-	RU	-
FI-N-100	30.6	9.85	-	RU	-
FI-N-150	30.6	9.32	-	RU	-
FI-N-200	30.6	9.12	-	RU	-
FI-B-25-1	30.6	12.62	-	RU	12.91
FI-B-25-2	30.6	13.20	-	RU	
FI-B-50	30.6	11.62	-	RU	-
FI-B-100	30.6	9.81	-	RU	-
FI-B-150	30.6	9.61	-	RU	-
FI-B-200	30.6	9.23	-	RU	-

*It should be noted that ultimate load applied to specimen CO-S-200 was not recorded properly and it was eliminated from analysis

[a]DB-C, debonding at adhesive-concrete interface with a layer of concrete attached to the debonded CFRP sheet; DB-I, debonding at adhesive-concrete interface without any layer of concrete attached to the debonded CFRP sheet; RU, CFRP rupture

Where β_w and β_l are dimensionless coefficients reflecting the effects of the FRP to concrete width ratio calculated using Eqs. (2) and (3), respectively. Additionally, b_c is width of concrete block and L_e is effective bond length, calculated using Eq. (4). Moreover, t_f, b_f, L_f and E_f are thickness, width, length and elasticity modulus of CFRP sheet, respectively. Based on the statistical analysis of test data obtained from other researchers, the best fit value was $\alpha = 0.427$.

Based on specification of the specimens and for mentioned equations, the calculated failure load for the specimens with concrete compressive strength of 29.7, 30.6 and 31.2 MPa estimated as 9.04, 9.18 and 9.27 kN, respectively.

4.1 Bond strength and failure modes

As shown in Fig. 8, the bond strength of wire brushed, sandblasted, and hole drilled specimens did not varry significantly. For specimens exposed to temperature of below epoxy resin T_g (T_g = 60℃), the bond strengths were not affected, but after passing T_g, bond strength significantly decreased. For example, the ultimate load for CO-B-50 and CO-B-25 were similar, but the ultimate load for CO-B-100 and CO-B-200 showed significant drop of 35% and 50%, respectively. Moreover, the failure mode of all specimens prepared by these three methods was CFRP

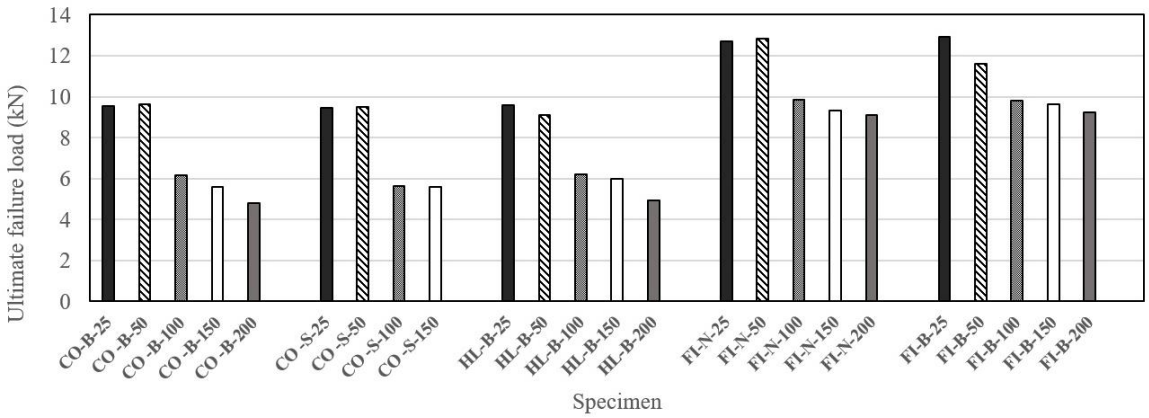

Fig. 8 Ultimate failure load of specimens

(a) Wire brushed specimen at 200℃ (b) Sandblasted specimen at 25℃ (c) Hole drilled specimen at 50℃

Fig. 9 Failure modes of wire brushed, sandblasted and hole drilled specimens. CFRP debonding at adhesive-concre interface with or without layer of concrete attached to the debonded CFRP sheet

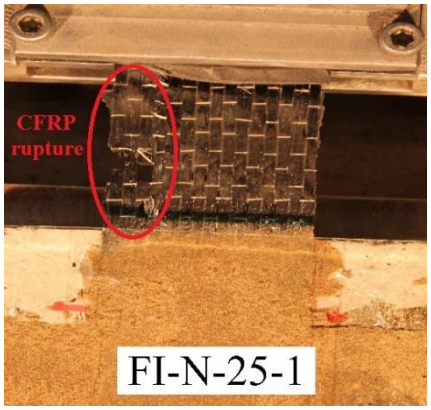

Fig. 10 Failure mode of fiber implanted specimen at 25 ℃: CFRP rupture

debonding at adhesive-concrete interface. For specimens exposed to the temperatures of 25 and 50℃ the failure mode was CFRP debonding at adhesive-concrete interface with a thin layer of concrete attached to the debonded CFRP sheet and for specimens exposed to the temperatures of 100, 150 and 200℃ the failure mode was CFRP debonding at adhesive-concrete interface without any concrete stripped off (Fig. 9).

The results for fiber implanted specimens were similar to each other (both systems with and without surface preparation). The fiber implantation method led to 32% increase in bond strength compared to conventional method for unexposed specimens. For specimens exposed to elevated temperatures, use of fiber implantation method was more productive. For example, the ultimate load for FI-N-200 was increased by 90% compared with CO-B-200. Also, the failure mode of all fiber implanted specimens was CFRP rupture (see Fig. 10).

By comparing the predicted ultimate load of Chen and Teng's model with present experimental results, it was evident that this model well predicted the bond strength for specimens prepared by different surface preparation methods (wire brushing, sandblasting and hole drilling) when being exposed to temperatures below resin T_g by should not be used for higher temperatures.

4.2 Load-displacement behavior

The load-displacement curves of all specimens were drawn using PIV analysis and presented in Fig. 11. Image analysis was used to determine the displacement at the loaded end of CFRP sheets during each test. In order to eliminate the rigid body motion-induced error of concrete

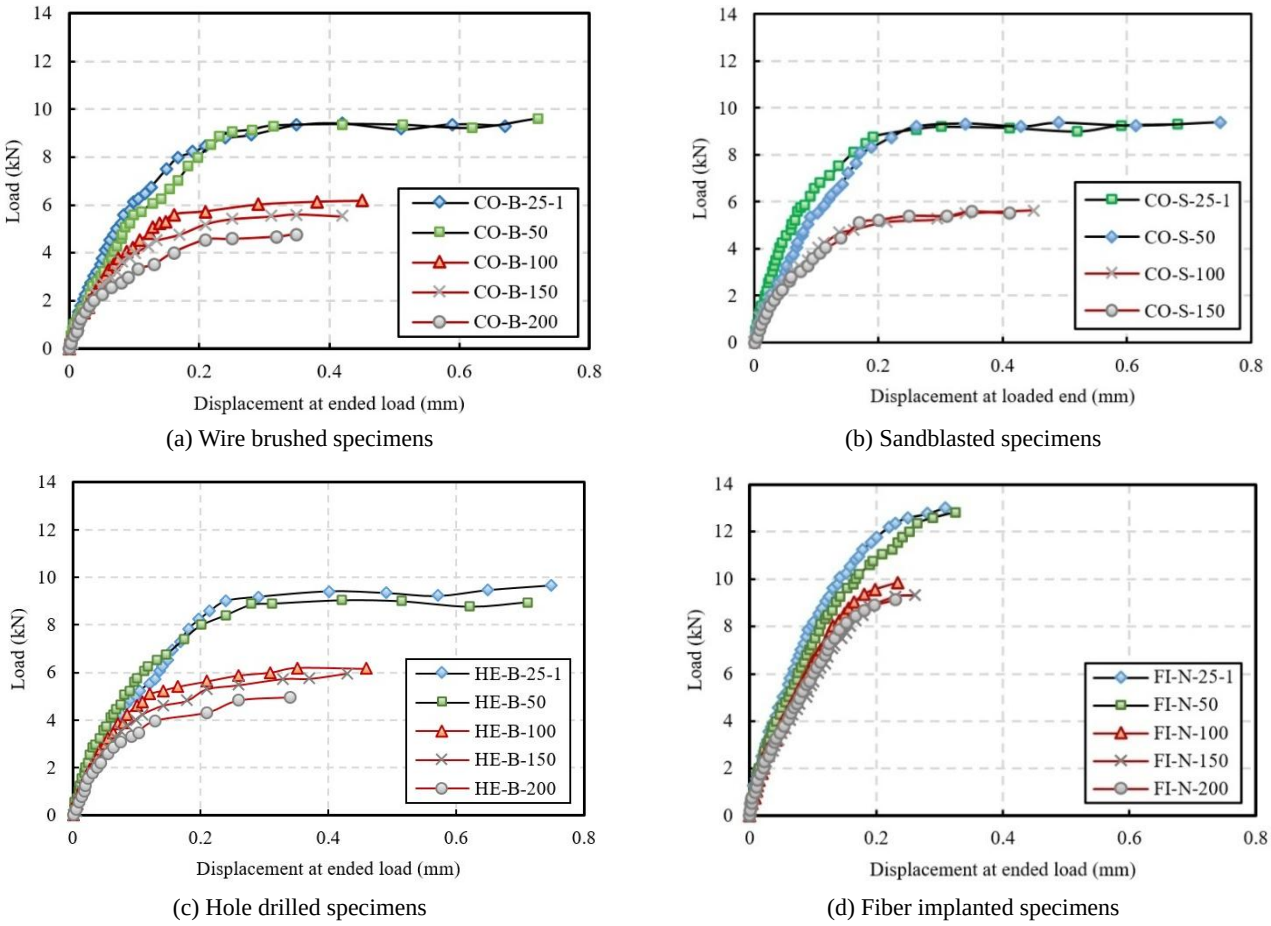

(a) Wire brushed specimens

(b) Sandblasted specimens

(c) Hole drilled specimens

(d) Fiber implanted specimens

Fig. 11 Load-displacement curves of specimens in various temperatures

specimens and elastic deformation of the support frame, the displacement of concrete block was also measured at each step and used in order to correct displacement calculations.

According to the results, the load-displacement curves of wire brushed, sandblasted and hole drilled specimens showed similar behavior. First, by increasing the load, the displacement increased proportionally and after reaching to about 95% of the ultimate load, the rate of increase in displacement significantly increased, as shown in Figs. 11(a) through 11(c). Therefore, longer bonded length did not lead to higher load carrying capacity, which was in agreement with the concept of effective bond length (the effective bond length of specimens based on the specification of specimens was 73 mm, which was calculated by Eq. (4)). It should be noted that by increasing temperature up to epoxy resin T_g, the behavior of load-displacement curve did not change. However, after passing this threshold, the initial slopes of the curves decreased and showed the reduction of stiffness in bonded region.

On the other hand, the load-displacement curves of fiber implanted specimens showed different behavior due to the change in the failure mode of fiber implanted specimens from CFRP debonding to CFRP rupture. The trend of the load-displacement curve was ascendant up to failure point. By increasing the temperature, the less reduction in slope and stiffness was observed compared to other methods (see Fig. 11(d)).

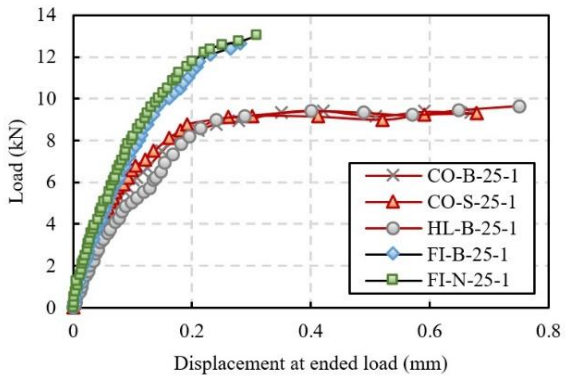

Fig. 12 Load-displacement curves of specimens at 25℃

Furthermore, if exposed temperature remained constant, the displacement of specimens which prepared by fiber implantation method was smaller and ultimate load increased. Fig. 12 showed this behavior for specimens exposed to the temperature of 25℃.

4.3 Strain distributions

The strain profiles of CO-B-25-1 and FI-N-25-1 specimens in different load levels were plotted using the results of PIV analysis. It is worth mentioning, based on the

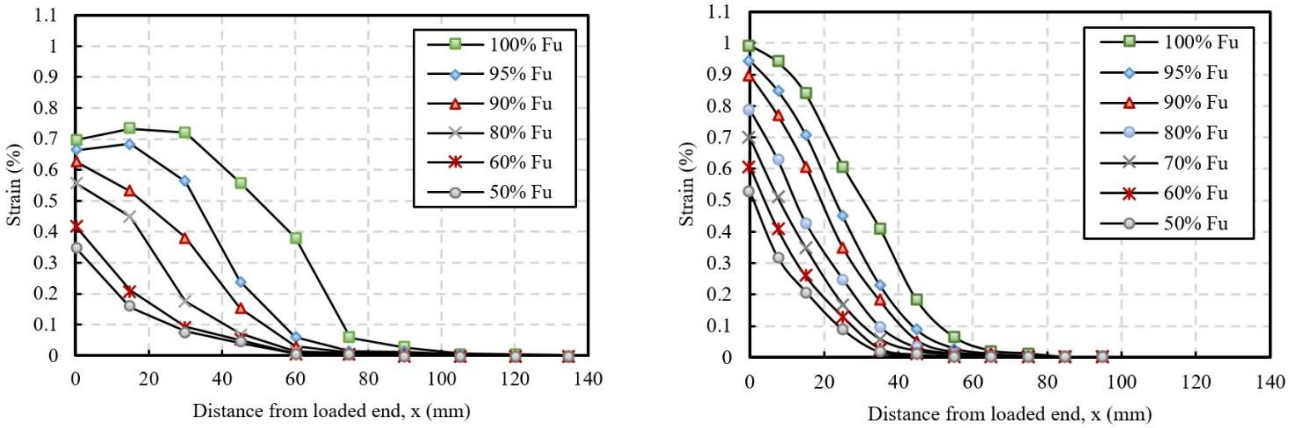

(a) Specimen CO-B-25-1 (b) Specimen FI-B-25-1

Fig. 13 Strain profiles corresponding to different load levels

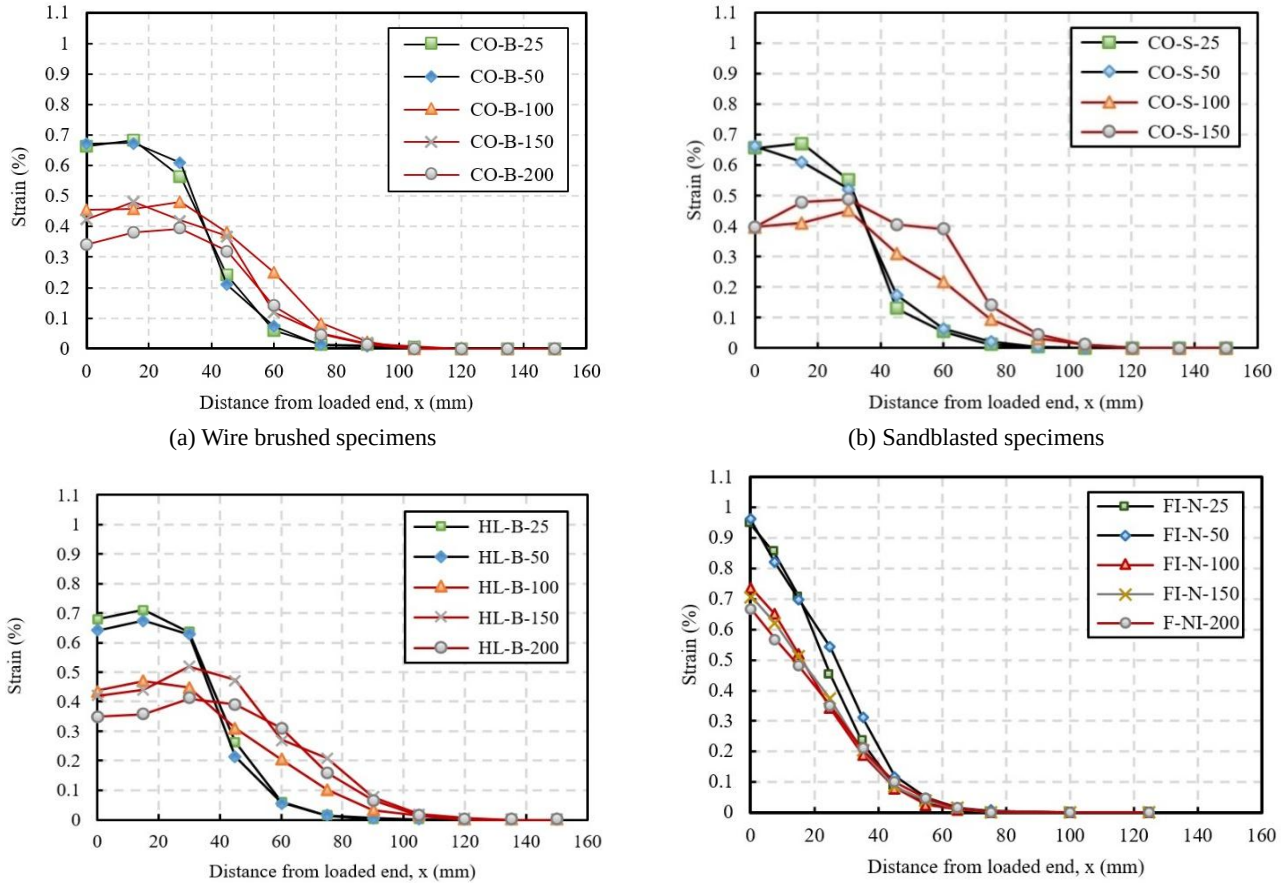

(a) Wire brushed specimens (b) Sandblasted specimens

(c) Hole drilled specimens (d) Fiber implanted specimens

Fig. 14 Strain profiles for different exposed temperature at 95% of ultimate load

study conducted by Yao *et al*. (2005), the strains at the loaded end of the specimens was calculated by dividing the applied stress by CFRP elasticity modulus. As shown in Fig. 13, the developed strains in the CFRP gradually decreased and eventually vanished at a distance referred to "effective bond length". Given the strain profile for CO-B-25-1, the applied force to CFRP sheet was transferred to the concrete block in the distance of about 75 mm (close to the to the effective bond length obtained by Chen and Teng's equation: 73 mm) for loading up to 95% of the final capacity. This distance was about 60 mm for FI-B-25-1 at the ultimate load capacity. Therefore, the fiber implantation method not only reduced the effective bond length by 20%, but also utilized the higher capacity of CFRP sheet.

In order to evaluate the effect of elevate temperature on the strain distribution pattern of CFRP sheet and effective

bond length, the strain profiles of specimens were plotted in different temperature at 95% of ultimate load in Fig. 14. As it can be seen, the specimens prepared by sandblasting, wire brushing, and hole drilling methods did not display much significant change in the strain distribution pattern and the effective bond length below epoxy resin T_g. However, by passing this threshold, the strain distribution pattern changed throughout the CFRP sheet and the effective bond length of CFRP sheet increased. For example, the effective bond length of CO-B-200 was 90 mm, which was 20% higher than that related to CO-B-25.

As it is illustrated in Fig. 14(d), fiber implanted specimens, when exposed to temperatures above resin epoxy T_g, did not show any change in the effective bond length and strain distribution pattern while carry smaller ultimate strain.

5. Conclusions

In this research, effects of exposure to elevated temperature and type of surface preparation on bond strength between externally bonded CFRP sheets and concrete substrate were investigated. Surface preparation methods considered in this study were sand blasting, wire brushing, hole drilling, and fiber implantation (as proposed method). In addition, evaluated temperatures of 25, 50, 100, 150, and 200℃ were considered. A total of 30 concrete specimens were prepared and exposed to different temperatures. The specimens were tested using near-end supported single-shear pull test at 25℃. Also, an image-based deformation measurement technique, referred as particle image velocimetry (PIV), was used to measure CFRP-concrete bond deformation of specimens. Based on evaluations carried out in the present study, the following conclusions could be drawn:

- Bond strength and stiffness of specimens prepared by three conventional methods of sandblasting, wire brushing and hole drilling did not vary significantly and they were not reduced up to resin epoxy T_g, however, beyond resin epoxy T_g, the bond strength and stiffness were significantly reduced. Average bond strength of sand blasted and wire brushed specimens exposed to temperatures of 100℃, 150℃, and 200℃ was reduced 38%, 41%, and 50% compared to control specimen kept at 25℃, while, the average bond strength of tested specimens at 50℃ remained unchanged (0.6%) compared to the tested specimen at 25℃.
- The bond strength of fiber implanted specimens was similar in both systems (with and without surface preparation). These values for specimens exposed to temperatures of 25℃, 50℃, 100℃, 150℃, and 200℃ displayed 32%, 33%, 59%, 66%, and 90% increase compared to conventional specimens, respectively. Besides, the failure mode of all specimens was CFRP rupture, which showed the ability of this method to utilize much higher capacity of CFRP sheet. Therefore, using fiber implantation could be a good and effective technique for external bonding of FRP sheets, especially when exposed to elevated temperatures.
- The bond strength and effective bond length for three conventional methods of wire brushing, sandblasting and hole drilling agreed as well with values obtained from Chen and Teng's equation up to epoxy resin T_g. Beyond this point, bond strength and effective bond length could not be estimated by their model.
- The effective bond lengths for specimens prepared with conventional method were 75 mm and 90 mm for specimens unexposed and exposed to 200℃, respectively. These values were reduced to 60 mm and 65 mm, respectively, when fiber implantation technique was used. This demonstrates the efficiency of proposed method, especially in externally bonded FRP systems exposed to temperatures.

Acknowledgments

This research was supported by faculty of engineering at Ferdowsi University of Mashhad under research grant No. 41801. The authors are grateful for the support from civil engineering department and thankful for the help provided by staffs of structures laboratory where the experiments were carried out.

References

Adrian, R.J. (1991), "Particle-imaging techniques for experimental fluid mechanics", *Annual Rev. Fluid Mech.*, **23**(1), 261-304. https://doi.org/10.1146/annurev.fl.23.010191.001401

Ali-Ahmad, M., Subramaniam, K. and Ghosn, M. (2006), "Experimental investigation and fracture analysis of debonding between concrete and FRP sheets", *J. Eng. Mech.*, **132**(9), 914-923. https://doi.org/10.1061/(ASCE)0733-9399(2006)132:9(914)

Al-Salloum, Y.A., Elsanadedy, H.M. and Abadel, A.A. (2011), "Behavior of FRP-confined concrete after high temperature exposure", *Constr. Build. Mater.*, **25**(2), 838-850. https://doi.org/10.1016/j.conbuildmat.2010.06.103

ASTM D3039M-00 (2000), Standard test method for tensile properties of polymer matrix composite materials.

Barros, J.A.O. and Fortes, A.S. (2005), "Flexural strengthening of concrete beams with CFRP laminates bonded into slits", *Cement Concrete Compos.*, **27**(4), 471-480. https://doi.org/10.1016/j.cemconcomp.2004.07.004

Blontrock, H. (2003), "Analysis and modeling of the fire resistance of concrete elements with externally bonded FRP reinforcement", Ph.D. Thesis; Ghent University, Ghent, Belgium.

Burke, P.J., Bisby, L.A. and Green, M.F. (2013), "Effects of elevated temperature on near surface mounted and externally bonded FRP strengthening systems for concrete", *Cement Concrete Compos.*, **35**(1), 190-199. https://doi.org/10.1016/j.cemconcomp.2012.10.003

Carolin, A., Nordin, H. and Taljsten, B. (2001), "Concrete beams strengthened with near surface mounted reinforcement of CFRP", *Proceedings of International Conference on FRP Composites in Civil Engineering*, Amsterdam, Netherlands.

Chen, J. and Teng, J. (2001), "Anchorage strength models for FRP and steel plates bonded to concrete", *J. Struct. Eng.*, **127**(7),

784-791. https://doi.org/10.1061/(ASCE)0733-9445(2001)127:7(784)
Cheng, H.-L., Sotelino, E.D. and Chen, W.-F. (2002), "Strength estimation for FRP wrapped reinforced concrete columns", *Steel Compos. Struct., Int. J.*, **2**(1), 1-20. https://doi.org/10.12989/scs.2002.2.1.001
De Lorenzis, L. (2004), "Anchorage length of near surface mounted FRP bars for concrete strengthening – analytical modelling", *ACI Struct. J.*, **101**(3), 375-386.
Firmo, J.P., Correia, J.R. and Bisby, L.A. (2015a), "Fire behaviour of FRP-strengthened reinforced concrete structural elements: a state-of-the-art review", *Compos. Part B: Eng.*, **80**, 198-216. https://doi.org/10.1016/j.compositesb.2015.05.045
Firmo, J.P., Pitta, D., Correia, J.R., Tiago, C. and Arruda, M.R.T. (2015b), "Experimental characterization of the bond between externally bonded reinforcement (EBR) CFRP strips and concrete at elevated temperatures", *Cement Concrete Compos.*, **60**, 44-54. https://doi.org/10.1016/j.cemconcomp.2015.02.008
Grace, N.F., Sayed, G.A., Soliman, A.K. and Saleh, K.R. (1999), "Strengthening reinforced concrete beams using fiber reinforced polymer (FRP) laminates", *ACI Struct. J.*, **96**(5), 865-874.
Hadji, L., Daouadji, T.H., Meziane, M. and Bedia, E. (2016), "Analyze of the interfacial stress in reinforced concrete beams strengthened with externally bonded CFRP plate", *Steel Compos. Struct., Int. J.*, **20**(2), 413-429. https://doi.org/10.12989/scs.2016.20.2.413
Hajialilue-Bonab, M., Azarnya-Shahgoli, H. and Sojoudi, Y. (2011), "Soil deformation pattern around laterally loaded piles", *Int. J. Phys. Model. Geotech.*, **11**(3), 116-125. https://doi.org/10.1680/ijpmg.2011.11.3.116
Hajihashemi, A., Mostofinejad, D. and Azhari, M. (2011), "Investigation of RC beams strengthened with prestressed NSM CFRP laminates", *J. Compos. Constr., ASCE*, **15**(6), 887-895. https://doi.org/10.1061/(ASCE)CC.1943-5614.0000225
Hosseini, A. and Mostofinejad, D. (2013), "Experimental investigation into bond behavior of CFRP sheets attached to concrete using EBR and EBROG techniques", *Compos. Part B: Eng.*, **51**, 130-139. https://doi.org/10.1016/j.compositesb.2013.03.003
Kim, Y.J., Hmidan, A., Choi, K. and Yazdani, S. (2012), "Fracture characteristics of notched concrete beams shear-strengthened with CFRP sheets subjected to high temperature", *ACI-Special Publication* (SP-286): A Fracture Approach for FRP-concrete.
Klamer, E.L. (2009), "Influence of temperature on concrete beams strengthened in flexure with CFRP", Ph.D. Thesis; Civil Engineering, Eindhoven University of Technology, Eindhoven, Netherlands.
Klamer, E.L., Hordijk, D.A. and Janssen, H.J. (2005), "The influence of temperature on the debonding of externally bonded CFRP", *Proceedings of 7th International Symposium on Fiber-Reinforced (FRP) Polymer Reinforcement for Concrete Structures*, New Orleans, LA, USA, November, pp. 1551-1570.
Klamer, E.L., Hordijk, D.A. and de Boer, A. (2007), "FE-analyses to study the effect of temperature on debonding of externally bonded CFRP", *Proceedings of 8th International Symposium on Fiber Reinforced Polymer Reinforcement for Concrete Structures* (*FRPRCS-8*), Patras, Greece, July.
Leone, M., Matthys, S. and Aiello, M.A. (2009), "Effect of elevated service temperature on bond between FRP EBR systems and concrete", *Compos. Part B Eng.*, **40**(1), 85-93. https://doi.org/10.1016/j.compositesb.2008.06.004
Malek, A.M., Saadatmanesh, H. and Ehsani, M.R. (1998), "Prediction of failure load of R/C beams strengthened with FRP plate due to stress concentration at the plate end", *ACI Struct. J.*, **95**, 142-152.
Mazzotti, C., Savoia, M. and Ferracuti, B. (2008), "An experimental study on delamination of FRP plates bonded to concrete", *Constr. Build. Mater.*, **22**(7), 1409-1421. https://doi.org/10.1016/j.conbuildmat.2007.04.009
Mostofinejad, D. and Hajrasouliha, M.J. (2010), "Experimental study on grooving detail for elimination of debonding of FRP sheets from concrete surface", *Proceedings of the 5th International Conference on FRP Composites in Civil Engineering*, Beijing, China, pp. 545-547.
Namrou, A.R. (2013), "An experimental investigation into the behavior of concrete elements rerofitted with NSM composite strips at elevated temperatures", M.Sc. Thesis; University of Colorado at Denver, Denver, CO, USA.
Nordin, H. and Taljsten, B. (2006), "Concrete beams strengthened with prestressed near surface mounted CFRP", *J. Compos. Constr., ASCE*, **10**(1), 60-68. ttps://doi.org/10.1061/(ASCE)1090-0268(2006)10:1(60)
Slominski, C., Niedostatkiewicz, M. and Tejchman, J. (2007), "Application of particle image velocimetry (PIV) for deformation measurement during granular silo flow", *Powder Technol.*, **173**(1), 1-18. https://doi.org/10.1016/j.powtec.2006.11.018
Spadea, G., Bencardino, F. and Swamy, R.N. (1998) "Structural behaviour of composite RC beams with externally bonded CFRP", *J. Compos. Constr., ASCE*, **2**(3), 132-137. https://doi.org/10.1061/(ASCE)1090-0268(1998)2:3(132)
White, D. and Take, W. (2002), "GeoPIV: Particle Image Velocimetry (PIV) software for use in geotechnical testing".
White, D., Take, W. and Bolton, M. (2003), "Soil deformation measurement using particle image velocimetry (PIV) and photogrammetry", *Geotechnique*, **53**(7), 619-631.
Wu, Z., Iwashita, K., Yagashiro, S., Ishikawa, T. and Hamaguchi, Y. (2005), "Temperature effect on bonding and debonding behavior between FRP sheets and concrete", *J. Soc. Mater. Sci.*, **54**(5), 474-480. https://doi.org/10.2472/jsms.54.474
Xin, H., Liu, Y. and Du, A. (2015), "Thermal analysis on composite girder with hybrid GFRP-concrete deck", *Steel Compos. Struct., Int. J.*, **19**(5), 1221-1236. https://doi.org/10.12989/scs.2015.19.5.1221
Yao, J., Teng, J. and Chen, J. (2005), "Experimental study on FRP-to-concrete bonded joints", *Compos. Part B: Eng.*, **36**(2), 99-113. https://doi.org/10.1016/j.compositesb.2004.06.001

CC